

# Effective Denoising and Adaptive Equalization of Indoor Optical Wireless Channel With Artificial Light Using the Discrete Wavelet Transform and Artificial Neural Network

Sujan Rajbhandari, *Student Member, IEEE*, Zabih Ghassemlooy, *Senior Member, IEEE*, and Maia Angelova

**Abstract**—Indoor diffuse optical wireless (OW) communication systems performance is limited due to a number of effects; interference from natural and artificial light sources and multipath induced intersymbol interference (ISI). Artificial light interference (ALI) is a periodic signal with a spectrum profile extending up to the MHz range. It is the dominant source of performance degradation at low data rates, which can be removed using a high-pass filter (HPF). On the other hand, ISI is more severe at high data rates and an equalizing filter is incorporated at the receiver to compensate for the ISI. This paper provides the simulation results for a discrete wavelet transform (DWT)—artificial neural network (ANN)-based receiver architecture for on-and-off keying (OOK) non-return-to-zero (NRZ) scheme for a diffuse indoor OW link in the presence of ALI and ISI. ANN is adopted for classification acting as an efficient equalizer compared to the traditional equalizers. The ALI is effectively reduced by proper selection of the DWT coefficients resulting in improved receiver performance compared to the digital HPF. The simulated bit error rate (BER) performance of proposed DWT-ANN receiver structure for a diffuse indoor OW link operating at a data range of 10-200 Mbps is presented and discussed. The results are compared with performance of a diffuse link with an HPF-equalizer, ALI with/without filtering, and a line-of-sight (LOS) without filtering. We show that the DWT-ANN display a lower power requirement when compared to the receiver with an HPF-equalizer over a full range of delay spread in presence of ALI. However, as expected compared to the ideal LOS link the power penalty is higher reaching to 6 dB at 200 Mbps data rate.

**Index Terms**—Adaptive equalization, artificial neural network (ANN), indoor optical wireless communication, wavelet denoising.

## I. INTRODUCTION

THE availability of licence free huge bandwidth in the infrared (IR) range can be effectively utilized for indoor and outdoor optical wireless (OW) communications. IR communications with a low cost and a small size transceiver together with a secure link operation has the potential to play a

major role in future personal communications [1], [2]. The ever increasing bandwidth requirement per user ( $> 10$  Mbps) and bandwidth congestion in the radio frequency (RF) systems have forced to look for alternative systems in certain applications. The RF communication systems, on the other hand, are technically more advanced offering more flexibility and mobility to end-users compared to the OW systems. Hence, OW systems may never replace RF-based schemes, but they certainly can operate in a complementary manner with preference depending upon the applications and environment. Relatively low cost, licence free secure link with immunity to electromagnetic interference and signal confinement within a room has made OW systems a viable solution for offering high data rates in a multitude of environments including university, railway stations, hospital, high-definition TV transmission within rooms, high-speed trains. OW systems using visible and IR light offers a bandwidth in range of THz, which, if fully utilized, would not require any wavelength multiple access techniques. On the other hand, cellular systems are relatively easy to implement in the IR domain offering high-performance with minimum inter-channel and adjacent channel interference since the cell coverage area can be specified precisely [3].

There has been a rapid industrial growth of application of both indoor and outdoor OW systems [2], [4], [5]. The outdoor OW links, also known as the free space optics (FSO), is already providing a commercial application in backbone long-haul communications using line-of-sight (LOS) links at data rates of more than 2.5 Gbps per wavelength [6], [7]. However, progress and development in the indoor application is relatively slow because of lack of mobility. However, the scenario is changing quickly largely due to the bandwidth congestion in the RF domain. Installation of optical hotspots in public buildings (rail way stations, airports, etc.) providing data rates in the range of GHz is already commercially available. The future office design will include high speed optical hotspot points in specific locations and for particular applications [1].

Basically three link topologies can be adopted for indoor applications: 1) LOS (directed and nondirected); 2) hybrid LOS; and 3) non-LOS. Directed LOS links requiring the least optical power and offering high data rates in excess of 1 Gbps is susceptible to blocking, restricts user mobility, thus requiring complex tracking systems [8]. Hybrid LOS systems provide mobility to a certain degree, but are less power efficient and suffers from blocking. Nondirected non-LOS (diffuse) topologies

Manuscript received February 20, 2009; revised May 01, 2009 and May 11, 2009. First published June 02, 2009; current version published August 28, 2009. This work was supported by Northumbria University.

S. Rajbhandari and Z. Ghassemlooy are with Optical Communication Research Group, School of CEIS, Northumbria University, Newcastle upon Tyne, NE1 8ST, U.K. (e-mail: fary.ghassemlooy@unn.ac.uk; sujan.rajbhandari@unn.ac.uk).

M. Angelova is with the Intelligent Modeling Lab, School of CEIS, Northumbria University, Newcastle upon Tyne, NE1 8ST, U.K. (e-mail: maia.angelova@unn.ac.uk).

Digital Object Identifier 10.1109/JLT.2009.2024432

provide mobility and are less susceptible to blocking; hence, it is the preferred option for indoor applications. However, diffuse links suffer from the multipath induced ISI, thus limiting the maximum achievable data rates, for example  $260 \text{ Mbps.m.s}^{-1}$  for a typical indoor OW system [9]. ISI also results in an additional power penalty that increases exponentially with the data rate.

In OW systems, signal degradation also arises from the ALI. The effect of ALI is more severe in indoor applications since the average transmitted optical power level is limited due to the skin and eye-safety considerations. The photocurrent at the receiver due to ALI is often greater than the signal current, thus causing severe degradation in the system performance. Without high-pass filtering, the optical power level required at the receiver for OOK is  $\sim 16 \text{ dBm/cm}^2$  irrespective of the bit rate [10]. An electrical high-pass filter (HPF) is incorporated in the receiver to remove the ALI; however, the use of the HPF in OOK systems provides insignificant improvements for data rates up to 10 Mbps [10]. HPF offers some improvement at higher data rates, but it introduces a form of ISI known as the baseline wander (BLW) effect, which is more severe for the baseband modulation techniques with a high-power spectral density (PSD) at the dc and low-frequency regions. Analog HPFs do not provide higher signal-to-noise ratio (SNR) gain; therefore, digital HPFs have been adopted in many systems [11]. However, the order of digital HPFs required for effective removal of ALI is  $>1000$  [11], thus making the system highly complex with a large delay time.

A receiver structure based on the continuous wavelet transform (CWT) and the artificial neural network (ANN) is studied in [11] for equalization and removal of ALI. The performance of the CWT-based receiver is comparable to a digital HPF with a cutoff frequency of 1 MHz. However, the problems associated with the CWT are: 1) a possibility of infinite scale with information overlaps between different scales, 2) the requirement to modify scales with changes in the data rate for optimum performance [11], 3) since the selection of scale is carried out visually then it is prone to human errors, and 4) system realization using CWT is extremely challenging. These short-falls of CWT can be overcome by utilizing a DWT without affecting the system performance. Since the scales are dyadic and filter banks composed of HPFs and low-pass filters (LPFs) are utilized for realization of DWT, the complexity is much reduced compared to the CWT and digital HPFs.

For highly dispersive channels, the power penalty associated with multipath propagation becomes critical at high data rates. ISI due to the multipath propagation can be mitigated to an extent by using an equalizing filter at the receiver. Both linear equalizer and decision feedback equalizer (DFE) are effective for reducing consequence of ISI in indoor applications, with the later displaying slightly improved performance. Since transmission channel parameters are not known in advance and the physical channel is time varying; adaptive algorithms are the preferred option. In this scenario, a training sequence is transmitted to approximate channel characteristics, and is used at the receiver to adjust equalizer's parameters accordingly. The equalizing algorithm assumes that the channel is linear; however, dispersion induced by the channel is nonlinear in nature [12]. The

received signal at each sampling instant may be considered as a nonlinear function of the past values of the transmitted symbols. Hence, if the channel is nonstationary, the overall channel response becomes a nonlinear dynamic mapping [12]. Thus, in time-varying environment, the equalization based on the filter is the non-optimum classification strategy as they have a linear decision boundary [13], [14]. The optimum strategy would be to have a nonlinear decision boundary. Recently, several equalizers based on the multilayer perceptrons (MLPs) and the recurrent neural network with a nonlinear decision boundary have been studied for adaptive equalization [13], [15]–[18]. In this paper, we have adopted MLP for equalization in indoor OW links.

In the presence of ALI, an equalizer is inadequate to provide improved system performance. ALI needs to be removed effectively before introducing equalizing filters. In this paper, a new method is proposed and studied for the compensation of adverse effect due to the ALI and ISI using the DWT and ANN, respectively. The ISI due to multipath propagation and ALI are often treated separately in the study of the indoor OW applications. This is due to the fact that one of them is the dominant source of system performance degradation. For example, for a low data rate  $<10 \text{ Mbps}$ , ALI is the main source of interference as the use of a HPF does not provide any significant improvement in performance, and multipath induced ISI is insignificant and hence can be ignored. On the other hand, at high data rates ( $>10 \text{ Mbps}$ ) and with inclusion of a HPF, ALI will have negligible effect on the performance in comparison to the ISI, which is the dominant source of interference. Though small, ALI also contributes to the performance degradation in the dispersive channel even at high data rates. Hence, simulations are carried out to examine the performance of OW systems employing a DWT-ANN-based receiver in a dispersive channel with ALI. Since DWT splits the signal into different frequency bands, the low-frequency noise can effectively be reduced by manipulating the DWT coefficients. On the other hand, ANN having the capability of forming a highly nonlinear decision boundary and with adaptability can be utilized in any physical transmission channels. Hence, the proposed system can practically be implemented in any physical channel.

The paper is organized as follows. A brief introduction to the diffuse indoor OW channel model is described in Section II. The basic concept of DWT denoising of ALI in indoor OW system is given in Section III as well as comparative studies of the power penalties for a LOS link employing DWT and HPF schemes. In Section IV, the ANN architecture for signal classification in a diffuse channel is presented. The performance of proposed DWT-ANN based receiver adopted for a diffuse channel with the ALI is presented in Section V with detail comparison with the HPF and a traditional equalizer for a range of data rates and delay spread. Finally, conclusions are given in the Section VI.

## II. INDOOR OPTICAL WIRELESS COMMUNICATION SYSTEMS

Due to the cost and complexity factors, the intensity modulated and direct detection (IM/DD) scheme is the only feasible modulation for indoor OW communications. In IM/DD, the intensity of optical source  $x(t)$  is directly modulated by the input signal. The photocurrent of the photodetector  $z(t)$  is directly proportional to the instantaneous power incident optical

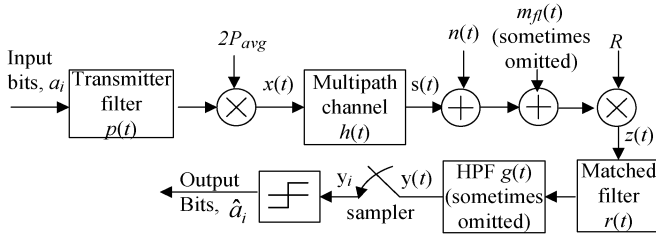


Fig. 1. Baseband model of a digital OW communication system.

signal (i.e., proportional to the square of received electric field). The complexity at the receiver is further reduced by introducing baseband modulation techniques such as OOK, pulse position modulation (PPM), digital pulse interval modulation (DPIM) [2], [19], [20]. The equivalent baseband indoor optical wireless model using OOK is shown in Fig. 1.

The input sequence  $a_i \in \{0, 1\}; i = 1, 2, \dots$  representing modulated signal is passed through a transmitter filter  $p(t)$  with a unit-amplitude impulse response of one slot duration  $T_b$  to convert it to a continuous signal. Hence, the output of the transmitting filter  $x(t)$  is given as

$$x(t) = A \sum_{i=-\infty}^{\infty} a_i p(t - iT_b) \quad (1)$$

where  $A$  is the amplitude of the signal.

The amplitude of the signal is scaled by the average optical power  $P_{avg}$  and transmitted through a multipath channel  $h(t)$ . The multipath propagation introduces delays between different signals arriving at the receiver from different paths, thus resulting in ISI. The signal dispersion caused by multipath propagation is modelled as a linear baseband impulse response  $h(t)$  [2]. Hence, the received signal  $s(t)$  in the absence of any noise is defined as

$$s(t) = x(t) \otimes h(t) \quad (2)$$

where the symbol  $\otimes$  denotes convolution. The optical signal is also corrupted by the background ambient noise due to artificial and natural lights, which is manifested in two different forms: the signal independent additive white Gaussian (AWG) shot noise and the interference introduced by the artificial light sources. ALI is deterministic and periodic with the potential of gravely impairing the link performance. The interference from a fluorescent light (FL) driven by an electronic ballast is the dominant cause of performance degradation as the interfering signal contains harmonics of the switching frequency that can extend into the MHz range [21]. An HPF is incorporated at the receiver to minimize the effect of the ALI. Without HPF, the input signal to the match filter is given by

$$z(t) = R[s(t) + n(t) + m_{fl}(t)] \quad (3)$$

where  $R$  is the photodetector responsivity,  $n(t)$  is the AWGN with zero-mean and variance of  $N_0/2$ , and  $m_{fl}(t)$  is the fluorescent induced photocurrent comprised of low and high-frequency components, details of which can be found in [22]. The amplitude of the photocurrent due to interference is often larger than that produced by the signal and the optical power requirements are approximately given by the inference amplitude [10].

The receiver incorporates a matched filter  $r(t)$ , matched to  $p(t)$ , with its output  $y(t)$  sampled at  $T_b = 1/R_b$ , where  $R_b$  is

the bit rate. Hence, the input signal to the decision device can be represented in a discrete form as

$$y_i = R[Aa_i \otimes h_k + n_k + m_k] \quad (4)$$

where  $h_k$  is the discrete-time impulse response for the system given by

$$h_k = p(t) \otimes h(t) \otimes r(t)|_{t=kT_b} \quad (5)$$

$n_k$  is given by

$$n_k = n(t) \otimes r(t)|_{t=kT_b} \quad (6)$$

and  $m_k$  is the sample output of the FL at the output of the matched filter given by

$$m_k = m_{fl}(t) \otimes r(t)|_{t=kT_b}. \quad (7)$$

The output of the matched filter  $y_i$  can be further processed using the equalizing filter and/or a digital HPF. In basic systems,  $y_i$  is converted into the binary “0” and “1” using a predefined threshold level to estimate the data sequence  $\hat{a}_i$ . The estimated data  $\hat{a}_i$  stream is compared to the transmitted data stream  $a_i$  to calculate the BER. In a LOS link without dispersion and ALI, the BER for OOK-NRZ with an optimum thresholding is given by

$$P_e = \frac{1}{2} Q \left( \frac{RP_{avg} \sqrt{T_b}}{\sqrt{N_0}} \right) \quad (8)$$

where  $Q(\cdot)$  is error function defined as  $Q(u) = (1/2\pi) \int_u^{\infty} e^{-v^2/2} dv$

Since the ALI is often periodic and deterministic, the BER in presence of ALI is estimated by averaging  $P_e$  over a interfering period and is given by [21]

$$P_e = \frac{1}{2M} \sum_{k=1}^M \left[ Q \left( \frac{RP_{avg} \sqrt{T_b} + m_k}{\sqrt{N_0}} \right) + Q \left( \frac{RP_{avg} \sqrt{T_b} - m_k}{\sqrt{N_0}} \right) \right] \quad (9)$$

where  $M$  is the total number of bits over a 20-ms interval.

In a dispersive channel, multipath induced ISI limits the maximum data rate that can be transmitted and also degrades the BER performance. The ISI at the decision bit depends on the transmitted bit pattern and the channel span  $L$ . The BER is approximated by averaging over all possible bits sequence of length  $L$ , and is given by

$$P_e = \frac{1}{2L} \sum_{i \in s_0} Q \left( \frac{a - y_i}{\sqrt{N_0}} \right) + \frac{1}{2L} \sum_{i \in s_1} Q \left( \frac{y_i - a}{\sqrt{N_0}} \right) \quad (10)$$

where  $s_0$  and  $s_1$  correspond to bit “0” and “1,” respectively.

The ISI induced power penalty is severe for links with data rates above 10 Mbps. At higher bit rates (100 Mbps or more) the power penalty incurred in a diffuse channel is so large, thus making it less practical without equalization. The power penalty in the diffuse channel is associated with the normalized delay spread  $D_T$  defined as

$$D_T = \frac{D_{rms}}{T_b} \quad (11)$$

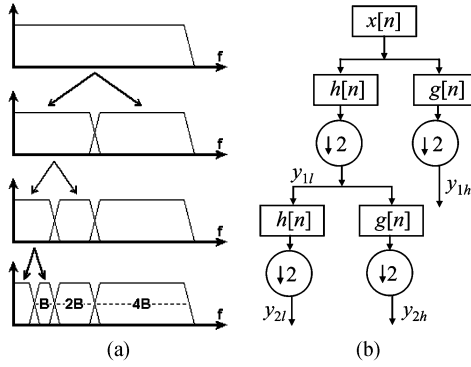


Fig. 2. (a) Decomposition of a signal by DWT (MRA), and (b) the decomposition process using high and low-pass filters.

where  $D_{\text{rms}}$  is the RMS delay spread related to the channel parameter  $a$  and channel impulse response  $h(t)$  follows [23]

$$D_{\text{rms}}(h(t, a)) = \frac{a}{12} \sqrt{\frac{13}{11}} \quad (12)$$

$$h(t, a) = \frac{6a^6}{(t+a)^7} u(t) \quad (13)$$

where  $u(t)$  is the unit step response,  $a = 2H/c$ ,  $H$  is the height between transmitter-receiver (Tx/Rx) and ceiling, and  $c$  is the speed of light.

For a comparative study of different systems, optical power required to achieve a certain BER,  $\text{BER}_0$  is used. In this paper, the optical power penalty (OPP) is defined in the equation at bottom of the page.

Here, a BER of  $10^{-5}$  is used for the standard BER and the ideal channel indicates a LOS AWGN channel without any interference.

### III. PERFORMANCE OF OOK IN LOS LINKS WITH DISCRETE WAVELET TRANSFORM

DWT is a multiresolutional analysis (MRA) tool in which signals are divided into half-frequency bands at each level of the decomposition as shown in Fig. 2. The practical implementation of the MRA can be done using a filter bank [24]. The signal is passed through a series of HPFs  $g[n]$  and LPFs  $h[n]$  to analyze the high and low-frequency components, respectively as illustrated in Fig. 2(b). The decomposition process involves the use of successive  $h[n]$  and  $g[n]$  to split the signal into its approximation and detail coefficients and down sampling by two. The outputs of the HPF and LPF  $y_h[k]$  and  $y_l[k]$ , respectively are given as [25]

$$y_h[k] = \sum_n x[n].g[2k-n] \quad (14)$$

$$y_l[k] = \sum_n x[n].h[2k-n]. \quad (15)$$

The HPF and LPF are associated with one another and satisfy the condition of a quadrature mirror filter, i.e., the sum of the magnitude response of HPF and LPF is equal to one for all frequencies as given by

$$g[J-1-n] = (-1)^n h[n] \quad (16)$$

where  $J$  is the filter length.

The approximation coefficients can further be decomposed into different DWT coefficient levels with a maximum level of  $\log_2 P$ , where  $P$  is the signal length. The reconstruction process involves reverse of the decomposition process. The signals at each level are up-sampled by two, passed through the synthesis filters  $g'[n]$  and  $h'[n]$  (HPF and LPF, respectively), and then added. However, the analysis and synthesis filters are the same, hence the reconstruction at each level is given by [11]

$$x[n] = \sum_k (y_{\text{high}}[k].g[2k-n]) + (y_{\text{low}}[k].h[2k-n]). \quad (17)$$

Flexibility with the DWT is that at each level of decomposition coefficients can be analyzed and manipulated separately. In the denoising process, DWT coefficients that correspond to the interference are manipulated in such a way that the reconstructed signal will be free from interference. In OW applications, the received signal  $y_i$  is mapped to different frequency bands and a frequency band corresponding to the ALI interference is removed from signal while reconstruction is performed. Since there is a frequency overlap between the ALI and OOK signals (with both signals having high PSD at a low-frequency region), it is not possible to denoise without losing some information about the signal. Hence, the denoising should be carried out in such a way to ensure that information lost is kept to a minimum level.

The DWT coefficients with 8th-level decomposition of the OOK signal at 100 Mbps and with ALI at a sampling time of 10 ns for both signals are depicted in Fig. 3. The photocurrent at the receiver due to ALI is assumed to be five times that of the signal. Since both the signal and ALI have significantly low-frequency components, the amplitude of approximation coefficients are large for both signal and interference as illustrated in Fig. 3. However, there is a clear difference in the detail coefficients with the ALI having almost zero values and the signal nonzero values. This difference in DWT coefficients can be utilized to remove the noise from the signal. In this paper, approximation coefficients are made zero at a certain level of decomposition and only the detail coefficients are retained in the decision-making process.

The received signal with ALI and the eye-diagrams of the received signal with ALI are illustrated in Fig. 4. For the reconstruction of the signal, the approximation coefficients at the 8th level of decomposition are made zero and the signal is reconstructed using the inverse process given in (17). The eye-diagram clearly shows the effectiveness of the wavelet denoising.

$$\text{OPP} = \frac{\text{Power require to achieve a BER}_0}{\text{Power require to achieve BER}_0 \text{ in an ideal chhanel @10 Mbps}}$$

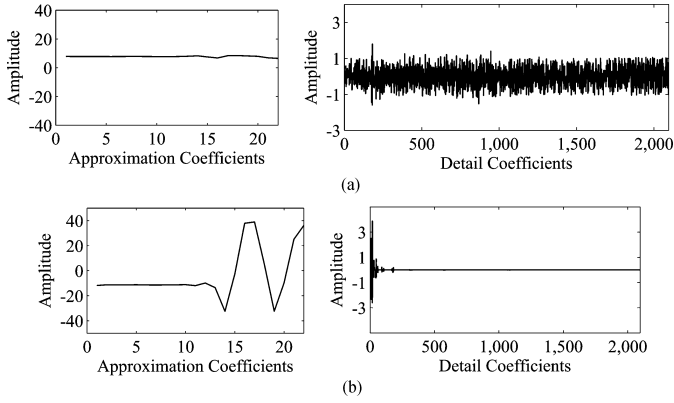


Fig. 3. Normalized DWT coefficient of (a) signal and (b) ALI.

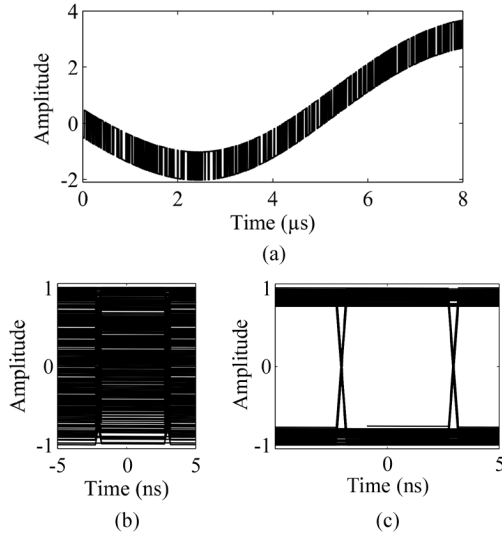


Fig. 4. (a) Received OOK signal in the presence of the FL interference, (b) the eye diagram of received signal corrupted by ALI (notice complete eye closer), and (c) the eye diagram of received signal with the wavelet denoising.

The complete eye closure in Fig. 4(b) is for the case of received signal with ALI, while the effect of denoising is clearly illustrated in the eye opening in Fig. 4(c). Further analysis of the effectiveness of the DWT can be done in terms of the OPP.

DWT offers flexibility in the analysis where different mother wavelets could be adopted. The OPPs linked to different mother wavelets are listed in Table I. Only selected mother wavelets from the Daubechies (db), Symlet (sym), discrete Meyer wavelet (dmey) biorsplines (bior), and Coiflets (coif) families with the best and the worst performance are listed. The Haar wavelet (db1) and the db8 show the worst and best performance, respectively, followed closely by the db10 and sym9. Hence, in all simulation results discussed hereafter, the db8 is used for DWT denoising.

Fig. 5 shows the OPP against the data rates for a LOS link and for four different scenarios: an ideal channel, ALI without filtering, ALI with a digital HPF, and ALI with DWT denoising. In [11] it is shown that the analog HPF displays much inferior performance compared to the digital HPF; hence, it is not considered in this study. The digital HPF comprises of an equiripple FIR filter with the cutoff and passband frequencies of 0.5 MHz and 1 MHz, respectively. The number of decomposition levels  $K$  for the DWT is calculated using:

$$K = -\lceil \log_2(T_s \times 0.5E6) \rceil \quad (18)$$

TABLE I  
OPTICAL POWER PENALTY ASSOCIATED WITH MOTHER WAVELETS FOR IN LOS LINKS IN PRESENCE OF ALI USING OOK AT 200 Mbps WITH DWT DENOISING

Mother Wavelets	Optical Power Penalty
db1	12.42
db2	11.40
db8	11.13
db10	11.14
dmey	11.24
Sym1	12.36
Sym4	11.19
Sym9	11.21
coif1	11.43
Coif5	11.70
bior2.2	11.27

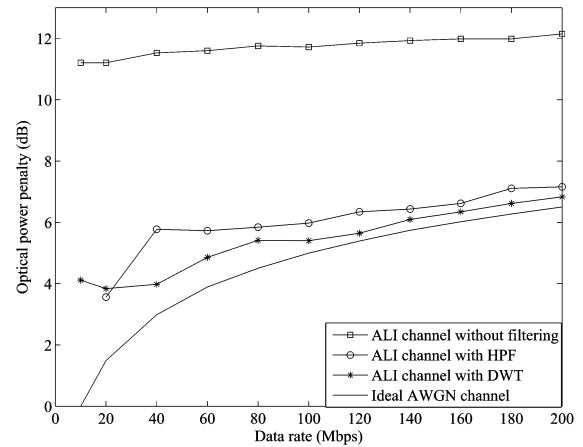


Fig. 5. Optical power penalty against data rate for OOK for a LOS link with AWGN and ALI with/without filtering at a BER of  $10^{-5}$ .

where  $\lceil x \rceil$  is the ceiling function. The cutoff frequency  $f_c$  for the DWT is also made equal to  $\sim 0.5$  MHz to match with the HPF. DWT shows marginally lower OPPs ( $\sim 0.5-1$  dB) and higher OPPs ( $< 0.5$  dB) compared to the HPF and the ideal channel, respectively, at higher data rates of  $> 20$  Mbps (see Fig. 5). In [11], it has been reported that at higher data rates, the CWT-ANN system displays marginally lower performance than the traditional receiver employing a filter with  $f_c$  of 1 MHz, showing  $< 1$  dB penalty for a filter with  $f_c$  of 0.5. In our study, we show that the DWT-based receiver outperforms a receiver employing a filter with  $f_c$  of 0.5 MHz.

The normalized OPPs against the decomposition levels  $K$  and the filter cutoff frequencies for a range of data rates (20, 50, 100, and 200 Mbps) for HPF- and DWT-based receivers, respectively, at a BER of  $10^{-6}$  is depicted in Fig. 6. The OPPs are normalized to that of an ideal channel for the same data rates. Both plots display threshold (optimum) levels beyond which the OPP increases exponentially. For DWT the lowest threshold level is at  $K = 9$  for 200 Mbps. Since DWT decomposes signal in a logarithmic scale, the value of  $K$  at which OPP is minimal increases by one when the data rate doubles. In case of the HPF, the optimum cutoff frequency is  $\sim 0.2$  MHz for all data rates. Note, it is not possible to define precise cutoff frequencies for DWT (as only the integer value of  $K$  is possible). The results shown in Fig. 6 indicate that the wavelet-based receiver, with no

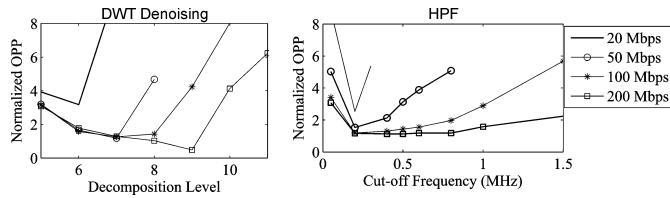


Fig. 6. Normalized optical power penalty against the decomposition level and cutoff frequencies for a HPF- and DWT-based receivers at data rates of 20, 50, 100, and 200 Mbps.

parameter optimization, displays similar or better performance compared to the best achieved with the HPF. This makes the denoising process faster and more convenient.

In addition to the performance improvement, a key advantage of the DWT is the reduced system complexity. For the optimum performance, the value of  $K$  varies from 6–9 (Fig. 6). For the input signal length of  $n$ , the total number of floating point operations (only multiplication is taken into consideration here) for the first level of decomposition is  $nJ$ . For the second stage, the length of input signal is  $n/2$  and the total number of operations is  $nJ/2$  and so on. Hence, the DWT requires a maximum of  $2nJ$  operations for analysis and synthesis meaning the maximum number of floating point operations is  $4nJ$ . Since  $J = 15$  for Daubechies 8 “db8,” the maximum number of the operations is  $60n$ . For an HPF of order  $L$ , the total number of floating point operations is  $nL/2$ . At a data rate of 200 Mbps and with a  $f_c$  of 0.2 MHz, the filter order is 2148, thus illustrating much reduced complexity of the DWT. Moreover, the realization of the DWT is also simpler compared to the HPF as a repetitive structure is used at each level of analysis and synthesis. Hence, only a 15th-order filter is required to realize for the DWT compared to a filter of 2148 orders for the HPF.

#### IV. ANN-BASED EQUALIZER

The multipath induced ISI limits the unequalized data rates that can be achieved. Beyond certain data rates, the power penalty due to the ISI becomes considerably large for any practical applications; hence, an equalizer is incorporated at the receiver to compensate for the ISI induced power penalty. Traditionally, a digital filter with adjustable tap coefficients was used for the equalization. The adaptive equalization techniques, in which channel parameters are estimated at the receiver by transmitting a training sequence, are widely used in practical channels [26]. Recently ANN-based equalizers have been extensively studied as ANN provides more flexibility and robustness. The main characteristic that makes the ANN very attractive for the channel equalization is its ability of forming a nonlinear decision boundary, which is the optimum for equalizing a time-varying channel [13], [15]. The adaptability, parallel processing, self-organization, universal approximation, and the capability of tackling a highly nonlinear problem are other advantages of the ANN when compared to the traditional equalizers.

The structure of an ANN-based DFE is depicted in Fig. 7. As in traditional DFE, there are feed-forward and feedback loops. With no feedback loop the structure would be equivalent to a traditional linear equalizer. The ANN used in this study is the feed-forward back-propagation multilayer perceptrons with supervised training. As in other adaptive equalization schemes,

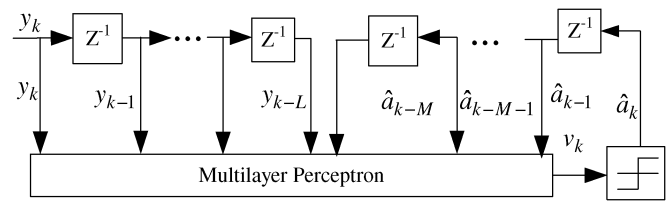


Fig. 7. ANN-based DFE structure.

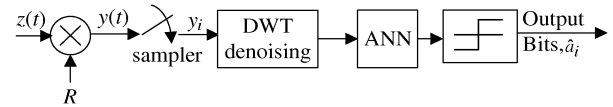


Fig. 8. Block diagram of the DWT-ANN-based receiver for an indoor OW link for removal of the ALI and equalization.

channel parameters are approximated by transmitting a training sequence which are used to adjust the ANN free parameters to minimize the difference between target and actual outputs. However, the concept of equalization is different from the traditional channel compensation mechanisms. With ANN, the task of the receiver is to classify the received signal vector in one of the two classes: binary 0 and binary 1. The effectiveness of the ANN as a classifier depends upon the training sequence and the training algorithms. ANN is capable of compensating for the ISI even in a highly dispersive and time-varying channel, outperforming the traditional equalizers for both linear and nonlinear channels [12], [27]. In the case of indoor OW applications, ANN equalizers show identical performance to the traditional equalizers for all channel conditions [28], [29] and therefore these results will not be reported here.

#### V. DWT-ANN-BASED RECEIVER IN DIFFUSE LINKS WITH ALI

The receiver block diagram of an OW link employing the DWT-ANN equalizer is illustrated in Fig. 8. The receiver structure is similar to the traditional structure with the DWT and ANN replacing the traditional HPF and the adaptive equalization. For channels with no ALI, the DWT block can be removed without degradation in the system performance. However, with no HPF or DWT there is no improvement in the performance, this is because ALI is the dominating source of noise. Simulations are carried out for comparative studies of the DWT-ANN based receiver and a HPF-traditional FIR filter equalizer under the same channel conditions. All the major simulation parameters for both systems are tabulated in Table II.

Fig. 9 shows the optical power penalty at a BER of  $10^{-5}$  over a range of data rates for indoor OW links (LOS and diffuse) with  $D_{\text{rms}}$  of 10 ns. DWT-ANN and HPF-FIR equalizers are only used for the diffuse links. For comparison, the optical power penalty for a LOS link with an ideal AWGN channel without ALI, the unequalized system without ALI and an ANN equalizer with no ALI are also shown. At a low data rate region ( $<20$  Mbps) with no ALI, the optical power penalty is the lowest ( $<2$  dB) for an ideal LOS link and a diffuse link with/without an ANN equalizer. The diffuse link with no equalizer displays an exponential raise in the power penalty. At higher data rates, as expected, the LOS link power penalty is the lowest reaching  $\sim 6.5$  dB at a data rate of 200 Mbps compared to all other cases. The ALI interference can be effectively reduced

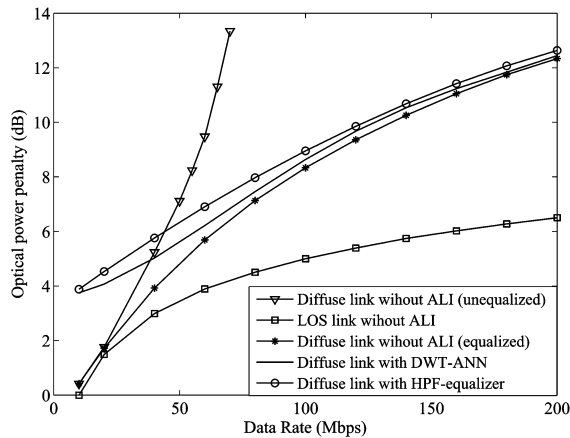


Fig. 9. Optical power penalty at a BER of  $10^{-5}$  over a range of data rates for indoor OW links (LOS and diffuse) with  $D_{rms}$  of 10 ns and DWT-ANN and HPF-equalizer receivers (diffuse links).

TABLE II  
SIMULATION PARAMETERS

Parameters	Value
Data rate $R_b$	10-200 Mbps
Channel delay spread $D_{rms}$	10 ns
Mother wavelet	db8
ANN type	Feedforward back propagation
No. of neural layers	2
No. of neurons in 1 <sup>st</sup> layer	6
No. of neurons in 2 <sup>nd</sup> layer	1
ANN activation function	Log-sigmoid, linear
ANN training algorithm	Levenberg-Marquardt optimization
Training length	4000
HPF type	equiripple
Cut-off frequency	0.5 MHz
Passband frequency	1 MHz

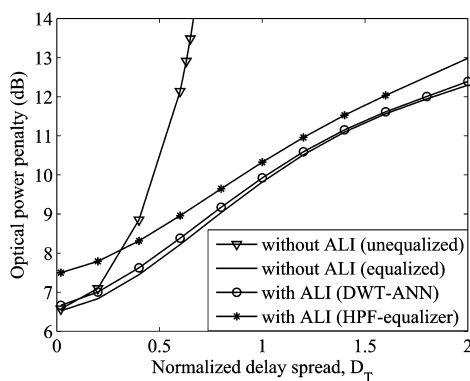


Fig. 10. Optical power penalty against the normalized delay spread for diffuse indoor links with/without ALI and equalizer at a BER of  $10^{-5}$  and a data rate of 200 Mbps.

using either DWT-ANN or HPF equalizers even for the diffuse link. At high data rates ( $>80$  Mbps) the DWT-ANN displays marginally lower and higher power requirement compared to the HPF-equalizer receiver and the ANN equalizer with no ALI, respectively. However, compared to the ideal LOS link the power penalty is high reaching 6 dB at 200 Mbps data rate.

Fig. 10 illustrates the optical power penalty for a range of  $D_T$  at a data rate of 200 Mbps and a BER rate of  $10^{-5}$  for equalized and unequalized systems with/without ALI. The system with no equalization shows the worst power penalty increasing exponentially at  $D_T > 0.25$ , thus resulting in irreducible BERs. Both DWT-ANN with ALI and ANN with no ALI display a lower-power requirement when compared to the receiver with a HPF-equalizer over the full range of  $D_T$ . For  $D_T = 0.2$  the equalized and DWT-ANN systems offer a 0.5-dB power advantage over the unequalized case increasing to  $>1$  dB at  $D_T$  of 0.4.

## VI. CONCLUSION

A receiver structure based on the DWT and ANN was introduced for effective removal of the ALI and multipath induced ISI in indoor OW links. At the receiver, by properly manipulating the DWT coefficients the effect of the ALI is minimized, whereas ISI effect is reduced by means of the ANN-based channel compensator. The simulation results obtained illustrated that the proposed receiver is highly effective in reducing the ALI and ISI, with performance surpassing the traditional HPF-equalizer-based receiver schemes in the presence of FLI. In LOS links, the DWT provides an improved performance compared to the HPF and marginally inferior performance compared to the channel without ALI. In the dispersive channel with ALI, results showed that the DWT-ANN receiver provides the best performance offering SNR gain of  $<0.5$  dB compared to the HPF-equalizer receiver. In fact, the DWT-ANN system in presence of ALI in a diffuse channel can closely match the performance of a link with no ALI. In addition to the performance improvement, further key advantages of the DWT-ANN based receiver compared to the traditional receiver structures are the reduced system complexity and increased flexibility. The DWT-based denoising scheme is able to match the best performance obtained using the HPF without the need for parameter optimization. The system has the potential to be applicable to other digital communication systems though this study was limited to the indoor OW applications.

## REFERENCES

- [1] D. O'Brien, G. Parry, and P. Stavrinou, "Optical hotspots speed up wireless communication," *Nature Photon.*, vol. 1, no. 5, pp. 245–247, 2007.
- [2] R. J. Green, H. Joshi, M. D. Higgins, and M. S. Leeson, "Recent developments in indoor optical wireless systems," *IET Commun.*, vol. 2, no. 1, pp. 3–10, 2008.
- [3] P. L. Eardley, D. R. Wisely, D. Wood, and P. McKee, "Holograms for optical wireless LANs," *IEE Proc. Optoelectron.*, vol. 143, no. 6, pp. 365–369, 1996.
- [4] "Free Space Optics (FSO): An Introduction." [Online]. Available: <http://www.free-space-optics.org>, last access data, Feb. 18, 2009.
- [5] "IrDA Market Report 2007." [Online]. Available: [http://www.irda.org/associations/2494/files/Publications/IrDA\\_MR\\_TOC.pdf](http://www.irda.org/associations/2494/files/Publications/IrDA_MR_TOC.pdf), last access data, Feb. 18, 2009.
- [6] D. M. Forin, G. M. Tosi Belefli, F. Curti, N. Corsi, V. De Sanctis, V. Sacchieri, A. J. L. Teixeira, and G. Cincotti, "On field test of a wavelength division multiplexing free space optics transmission at very high bit rates," in *Proc. 9th Int. Conf. Telecomm.*, 2007, pp. 77–80.
- [7] N. Cvijetic, D. Qian, and T. Wang, "10 Gb/s Free-Space Optical Transmission using OFDM," in *Proc. Opt. Fiber Commun./National Fiber Opt. Eng. Conf.*, San Diego, CA, 2008, pp. 1–3.
- [8] R. D. Wisely, "A 1 Gbit/s optical wireless tracked architecture for ATM delivery," in *IEE Colloquium Opt. Free Space Commun. Links*, London, U.K., 1996, pp. 14/1–14/7.
- [9] F. R. Gfeller and U. Bapst, "Wireless in-house data communication via diffuse infrared radiation," *Proc. IEEE*, vol. 67, no. 11, pp. 1474–1486, Nov. 1979.

- [10] A. J. C. Moreira, R. T. Valadas, and A. M. D. O. Duarte, "Performance of infrared transmission systems under ambient light interference," *IEE Proc. Optoelectron.*, vol. 143, no. 6, pp. 339–346, 1996.
- [11] R. J. Dickenson, "Wavelet analysis and artificial intelligence for diffuse indoor optical wireless communication," Ph.D. dissertation, School of CEIS, Northumbria Univ., Newcastle Upon Tyne, U.K., 2007.
- [12] J. C. Patra and N. R. N. Pal, "A functional link artificial neural network for adaptive channel equalization," *Signal Process.*, vol. 43, no. 2, pp. 181–195, 1995.
- [13] L. Hanzo, C. H. Wong, and M. S. Yee, "Neural network based equalization," in *Adaptive Wireless Transceivers*. New York: Wiley-IEEE Press, 2002, pp. 299–383.
- [14] P. Savazzi, L. Favalli, and V. Mecocci, "A suboptimal approach to channel equalization based on the nearest neighbor rule," *IEEE J. Sel. Areas Commun.*, vol. 16, no. 9, pp. 1640–1648, Dec. 1998.
- [15] A. K. Tripathy and K. T. Raghavendra, "An efficient channel equalizer using artificial neural networks," *Neural Netw. World*, vol. 16, no. 4, pp. 357–368, 2006.
- [16] B. Lu and B. L. Evans, "Channel equalization by feedforward neural networks," in *Proc. IEEE Int. Symp. Circuits Syst.*, 1999, vol. 5, pp. 587–590.
- [17] J. Choi, M. Bouchard, and T. H. Yeap, "Decision feedback recurrent neural equalization with fast convergence rate," *IEEE Trans. Neural Netw.*, vol. 16, no. 3, pp. 699–708, May 2005.
- [18] R. Zayani, R. Bouallegue, and D. Roviras, "Adaptive predistortions based on neural networks associated with Levenberg-Marquardt algorithm for satellite down links," *EURASIP J. Wireless Commun. Netw.*, vol. 2008, no. 5, pp. 1–15, 2008.
- [19] J. M. Kahn and J. R. Barry, "Wireless infrared communications," *Proc. IEEE*, vol. 85, no. 2, pp. 265–298, Feb. 1997.
- [20] J. B. Carruthers, "Wireless infrared communications," in *Wiley Encyclopedia of Telecommunications*. New York: Wiley, 2002.
- [21] R. Narasimhan, M. D. Audeh, and J. M. Kahn, "Effect of electronic-ballast fluorescent lighting on wireless infrared links," *IEE Proc. Optoelectron.*, vol. 143, no. 6, pp. 347–354, 1996.
- [22] A. J. C. Moreira, R. T. Valadas, and A. M. D. O. Duarte, "Characterisation and modelling of artificial light interference inoptical wireless communication systems," in *Proc. 6th IEEE Int. Symp. Personal, Indoor, Mobile Radio Commun.*, Toronto, ON, Canada, 1995, vol. 1, pp. 326–331.
- [23] J. B. Carruthers and J. M. Kahn, "Modeling of nondirected wireless Infrared channels," *IEEE Trans. Commun.*, vol. 45, no. 10, pp. 1260–1268, Oct. 1997.
- [24] S. G. Mallat, "A theory for multiresolution signal decomposition: The wavelet representation," *IEEE Trans. Pattern Anal. Mach. Intell.*, vol. 11, no. 7, pp. 674–693, Jul. 1989.
- [25] C. S. Burrus, R. A. Gopinath, and H. Guo, *Introduction to Wavelets and Wavelet Transforms: A Primer*. Englewood Cliffs, NJ: Prentice-Hall, 1998.
- [26] S. Haykin, "Adaptive digital communication receivers," *IEEE Commun. Mag.*, vol. 38, no. 12, pp. 106–114, Dec. 2002.
- [27] A. K. Pradhan, S. K. Meher, and A. Routray, "Communication channel equalization using wavelet network," *Digital Signal Process.*, vol. 16, no. 4, pp. 445–452, 2006.
- [28] S. Rajbhandari, Z. Ghassemlooy, and M. Angelova, "Performance of OOK with ANN equalization in indoor optical wireless communication system," in *Proc. PGNET 2007*, Liverpool, U.K., 2007, pp. 86–90.
- [29] S. Rajbhandari, Z. Ghassemlooy, and M. Angelova, "The performance of PPM using neural network and symbol decoding for diffused indoor optical wireless links," in *Proc. ICTON2007*, Rome, Italy, 2007, pp. 161–164.



**Sujan Rajbhandari** (M'03) received the B.S. degree in electronics and communication engineering from the Institute of Engineering, Pulchowk Campus, Tribhuvan University, Kathmandu, Nepal, in 2004 and the M.Sc. degree (with distinction) in optoelectronics and communication systems from Northumbria University, Newcastle upon Tyne, U.K., in 2005. He is currently pursuing the Ph.D. degree in optical wireless communications at Northumbria University for which he was awarded a University Ph.D. studentship.

His research interests lie in the area of optical communications and, more specifically, the application of artificial intelligence and wavelet transform for signal detection in optical wireless communication links.



**Zabih Ghassemlooy** (SM'02) received the B.Sc. (honors) degree in electrical and electronics engineering from the Manchester Metropolitan University, Manchester, U.K., in 1981, and the M.Sc. and Ph.D. degrees in optical communications from the University of Manchester Institute of Science and Technology (UMIST), in 1984 and 1987, respectively, with scholarships from the Engineering and Physical Science Research Council, UK.

From 1986 to 1987, he was a Demonstrator at UMIST, and from 1987 to 1988, he was a Postdoctoral Research Fellow at City University, London, U.K. In 1988, he joined Sheffield Hallam University as a Lecturer, becoming a Reader in 1995 and a Professor in Optical Communications in 1997. He was the Group Leader for Communication Engineering and DSP Subject, and also Head of the Optical Communications Research Group until 2004. In 2004, he moved to the University of Northumbria, Newcastle upon Tyne, U.K., as an Associate Dean for Research in the School of Computing, Engineering, and Information Sciences. He is also the Head of Northumbria Communications Research Laboratories. He was a Visiting Professor at the Ankara University, Ankara, Turkey, and Hong Kong Polytechnic University, and is currently a Visiting Professor at the Technological University of Malaysia. He is the Editor-in-Chief of The Mediterranean Journals of Computers and Networks, and Electronics and Communications. He serves on the Editorial Committees of a number of international journals, is the founder and the Chairman of the International Symposium on Communication Systems, Network, and DSP, a committee member of the International Institute of Informatics and Systemics, and a member of technical committee of a number of international conferences. He is a College Member of the Engineering, and Physical Science Research Council, U.K. (2003–2009), and has served on a number international research and advisory committees. His research interests are in the areas of photonic networks, modulation techniques, high-speed optical systems, and optical wireless communications. He has received a number of research grants from U.K. Research Councils, European Union, industry, and U.K. Government. He has published over 310 papers. He is a coeditor of an IET book on *Analogue Optical Fibre Communications* (IET, 1995), the proceedings of the CSNDSP 08, 06, and 98, and the 1st International Workshop on Materials for Optoelectronics 1995, U.K. He is the coeditor of a number of special issues: the IET Circuit, Devices, and Systems, August 2006, Vol. 2, No. 1, 2008, the Mediterranean Journal of Electronics and Communications on "Free Space Optics—RF," July 2006, the *IET Proceedings Journal* 1994, and 2000, and the *International Journal of Communications Systems* 2000.

Prof. Ghassemlooy was a recipient of the Tan Chin Tuan Fellowship in Engineering from the Nanyang Technological University, Singapore, in 2001. In 2006, he was awarded one of the best Ph.D. research supervisors at Northumbria University. From 2004–2006, he was the IEEE UK/IR Communications Chapter Secretary and the Vice-Chairman and currently is the Chairman. He is a fellow of the IET.



**Maia Angelova** received the B.Sc. (honors) degree in physics, the M.Sc. degree in theoretical physics, and the Ph.D. degree in mathematical and theoretical physics, all from Sofia University, Sofia, Bulgaria.

She is a Professor of mathematical physics and Head of the Intelligent Modelling Research Group, University of Northumbria, Newcastle upon Tyne, U.K. She was a Visiting Research Fellow at the University of Kent, Canterbury, from 1989 to 1991, a Lecturer in physics at Somerville College and member of Theoretical Physics at Oxford University from 1991 to 1996. She joined Northumbria University in 1997 as a Senior Lecturer, became a Reader in 2002, and Professor in 2004. She has research interests in the development and applications of group-theoretical and algebraic methods in condensed matter, dynamical systems in biology, bioinformatics, and mathematical models of communication networks. She has received funding from U.K. Research Councils, European Union, and a number of charities. She is a reviewer and panel member for the European FP5, FP6, and FP7, and member of Editorial Board of Bioinformatics and Biology Insights.

Prof. Angelova is a member of the IoP and LMS.